Aalborg Universitet

Mission profile resolution effects on lifetime estimation of doubly-fed induction generator power converter

Zhang, Guanguan; Zhou, Dao; Blaabjerg, Frede; Yang, Jian

Mission Profile Resolution Effects on Lifetime Estimation of Doubly-Fed Induction Generator Power Converter

Guanguan Zhang[a], Dao Zhou[b], Frede Blaabjerg[b], Jian Yang[a]

[a] *School of Information Science and Engineering, Central South University, Changsha, China*
[b] *Department of Energy Technology, Aalborg University, Aalborg, Denmark*

Abstract—In the wind energy generation system, mission profiles are complicated, which range from seconds to years. In order to estimate the consumed lifetime of the power converter, wind speed profiles with the time resolution of 1 hour, 1 second and 0.5 millisecond are studied in this paper, and the corresponding thermal modeling of power semiconductors are discussed. Accordingly, effects of different mission profiles on the consumed lifetime of the power converter are evaluated. In the above three thermal cycles, the IGBT of the grid-side converter and the diode of the rotor-side converter are more fragile, and the total consumed lifetimes are higher. Moreover, the short-term thermal cycles with milliseconds resolution induce the unbalance of the lifetime between the diode and IGBT of the grid-side converter, while thermal cycles with hour, second, and millisecond resolution consumes the similar lifetime of the power components in the rotor-side converter. Furthermore, it is concluded that the lifetime of power components reduces with the increased time resolution, especially for the rotor-side converter.

Keywords—doubly-fed induction generator system; lifetime estimation; multi-timescale thermal models;

I. INTRODUCTION

With respect to the power electronic systems, the power devices are the most frangible components [1], and their reliability issues are crucial to provide guidance for the design and maintenance of the system [2], [3]. Due to the higher efficiency and lower cost, the partial-scale power converter makes the Doubly-Fed Induction Generator (DFIG) more attractive in the wind power generation systems, and its reliability and the lifetime prediction has been studied [4][6].

However, a DFIG system consists of mechanical parts (such as wind turbine, yaw system) and the electronic parts (such as the generator, power converter, transformer), which avoidably contributes to the multi-timescale features. In this system, the power device switching, bandwidth of the current/voltage controller, thermal time constant of the device and cooling system, inertia of the turbine mechanical parts may vary from dozens of the micro-second to several minutes [7], which makes it challenging to have a unified thermal model to handle the annual wind profile. In order to solve this issue, a multi-timescale modeling of a photovoltaic system is studied in 0, which is established from the circuit-level, system-level, and environment-level. In respect to the DFIG system, the multi-timescale thermal models are established based on the different mission profiles, and the consumed lifetime based on the `chip solder fatigue` is discussed in this paper.

According to the mission profile with different time resolutions (such as 1 hour, 1 second and 0.5 millisecond), the multi-timescale thermal cycles can be derived, and then the consumed lifetime of DFIG power converter is calculated. Finally, the lifetime of the power components in the Back-to-Back (BTB) power converter is compared.

II. DFIG SYSTEM CONFIGURATION AND ITS MISSION PROFILE

A. Configuration of DFIG-Based Wind Power System

The configuration of the DFIG-based wind power system is shown in Fig. 1, the DFIG regulated by a BTB power converter provides the electrical energy from mechanical kinetic energy, where the cut-in speed is 4 m/s and the cut-off speed is 25 m/s in this study [9]. An input filter is applied to filter harmonics between the converter and power grid. For the BTB power converter, the Grid-Side Converter (GSC) is with one power module in each arm, while the Rotor-Side Converter (RSC) has two paralleled power modules in each arm, because of the higher rotor current and a lower rotor excitation voltage. Moreover, it is noted that each power module (containing two IGBTs and two diodes in a half bridge) has its own heatsink to simplify the following analysis.

B. Mission Profile

In order to analyze the effects of multi-timescale thermal models on the consumed lifetime of the DFIG power converter, the large, medium, and small timescales are defined within one year (with a step of 1 *h*), one hour (with a step of 1 *s*) and one second (with a step of switching period 0.5 *ms*), respectively. In the case of the large timescale, a field annual mission profile of wind speed and ambient temperature are given in Fig. 2(a) and (b), where the sample rate is 1 *h* and the average wind speed is 10 *m/s* belonging to the IEC class I. It can be seen that the wind speed and ambient temperature fluctuate with time, and these trends are stochastic to some extent.
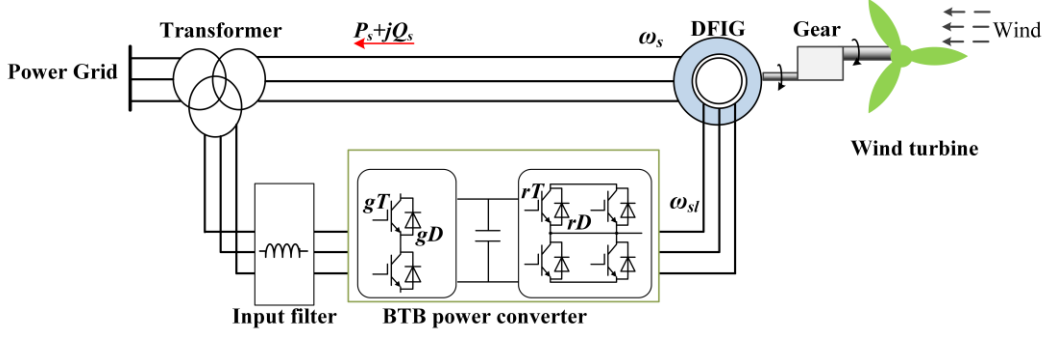
Fig. 1. The structure diagram of the DFIG system.

In order to obtain the mission profile related to medium timescale, the hourly wind speed with a time resolution of 1 s is regenerated by using

$$v(t) = v_h(t) + v_s(t) \qquad (1)$$

where $v_h(t)$ is the average wind speed within one hour, $v_s(t)$ is the turbulence component generated by the von Karman's spectra [10]. The generation process is given in Fig. 3, where the parameters calculation is discussed in [10], and the corresponding DFIG parameters are referring to the IEC standard. Fig. 4 shows the hourly mission profile of wind speed with v_h=10 m/s and the ambient temperature, where the ambient temperature is considered as a constant within 10 min and it can be extended to other average wind speeds to simplify the analysis.

For the small timescale with a period of 1 s, the wind speed and ambient temperature are constant considering their high time constants. The ambient temperature is the average value of annual mission profile and it is 9.5 ˚C all the time, while the wind speed is one of the cases among 1, 2, …, 28 m/s.
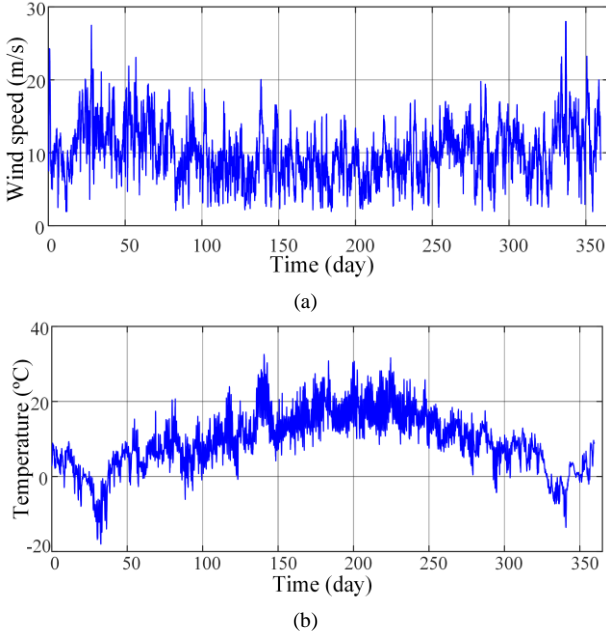
III. Consumed Lifetime Estimation with Multi-Timescale Thermal Models

From the viewpoint of the frequency domain, the thermal models of the power device and the heat sink are considered as the low-pass filters, and they feature with different time-scales. In this case, the long-term, medium-term and short-term thermal models are derived according to the above mission profiles, and the details are given as follows.

A. Lifetime Estimation at the Time Resolution of 1 h

Based on the mission profile shown in Fig. 2, the thermal cycles caused by the wind speed and ambient temperature fluctuations are the main factors, and the long-term thermal models are established as R impendence network model. Considering the large time-scale of 1 h, all the variables related to the DFIG system are in steady state, hence the output power

Fig. 3. Wind speed generation procedure.

(a)

(b)

Fig. 2. Yearly mission profile: (a) real-time wind speed, and (b) real-time ambient temperature.
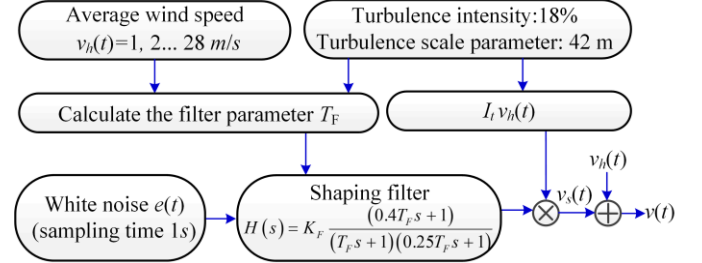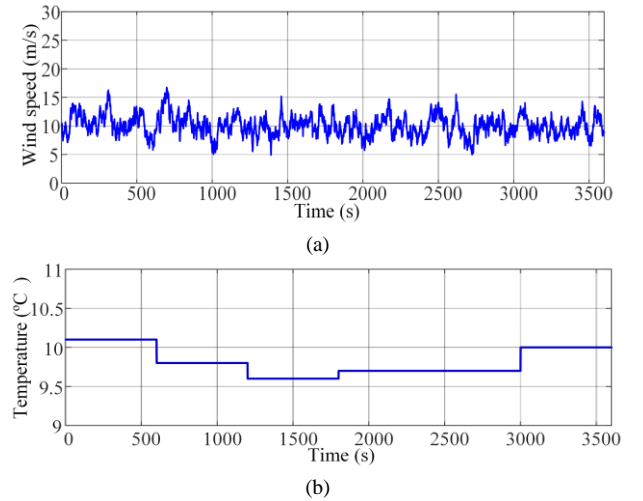

(a)

(b)

Fig. 4. Hourly mission profile with average wind speed of 10 m/s: (a) real-time wind speed, (b) real-time ambient temperature.
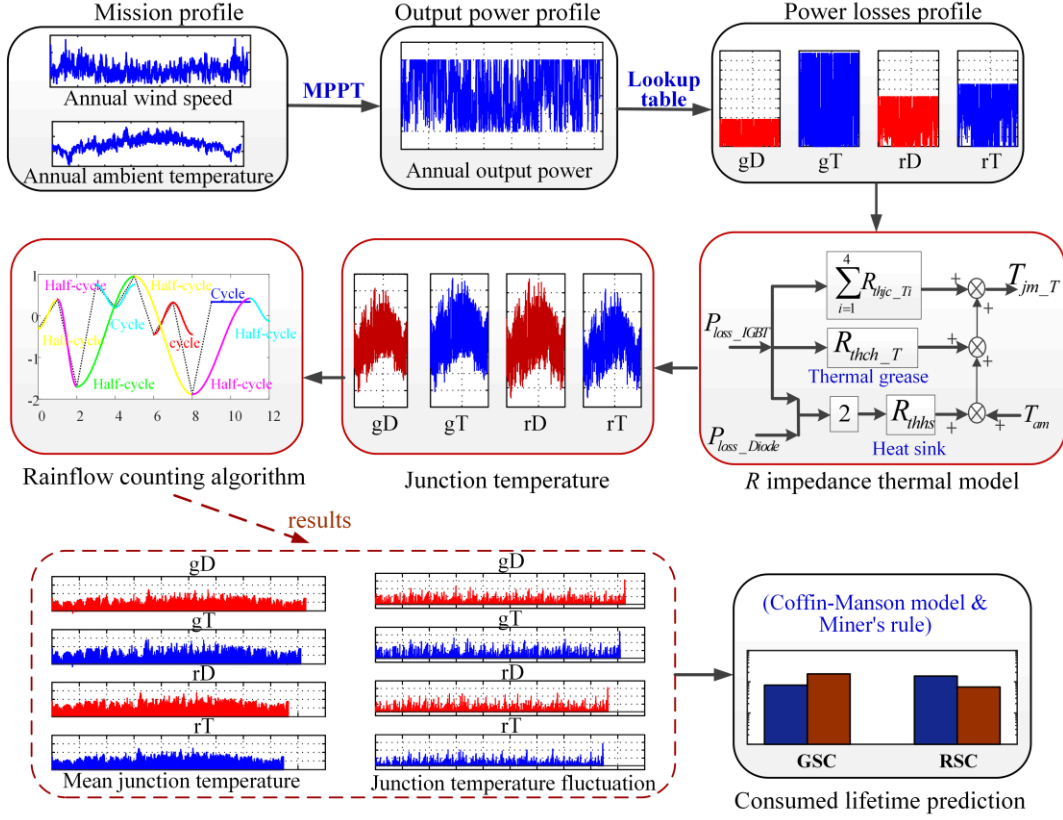
Fig. 5. The lifetime estimation procedure with the time resolution of 1 h.

curve meets the Maximum Power Point Tracking (MPPT) rule, and then the power losses of the power devices are obtained through the lookup table method.

The lifetime estimation procedure and the corresponding results are described in Fig. 5, where a rainflow counting algorithm is used to extract the thermal cycles with their average and swing values [11]. In the thermal impedance model in Fig. 5, R_{thjc}, R_{thch} and R_{thhs} are the thermal resistance from the junction to the case of the power module, the thermal grease and the heat sink, subscripts T and D denote the IGBT and the diode, respectively, subscripts i denote layer number, P_{loss} is the power loss of each power semiconductor, T_{am} is the ambient temperature. Based on the Coffin-Manson model and the Miner's rule, the lifetime of the DFIG power converter is calculated as

$$N_f = A \cdot dT_j^{\beta_1} \cdot e^{\frac{\beta_2}{273+T_{jm}(v)}} \cdot \left(\frac{t_{on}}{0.7} \right)^{\beta_3} \qquad (2)$$

$$CL = \sum CL_j = \sum \left(\frac{n_f(j)}{N_f(j)} \right) \qquad (3)$$

where N_f is the number of power cycles to failure, T_{jm} is the mean junction temperature, dT_j is the junction temperature fluctuation and t_{on} is the on-time duration. Besides, A, β_1, β_2, β_3 are fitting parameters based on test results provided by the manufacturer [12]. In (3), n_f is o.5 or 1 obtained from the rainflow counting algorithm, and j represents the jth calculated thermal cycles.

It can be seen that the power losses of the IGBT in the GSC and the RSC are the highest, while junction temperatures of IGBT and the diodes are similar. It is because that the thermal resistance of the diode is higher than that of the IGBT, and the total power losses between the GSC and the RSC are relatively balanced. On the other hand, for the power components of the GSC, the thermal cycles obtained from rainflow counting method are larger than that in RSC, which also contributes to the total consumed lifetime of GSC.

B. Lifetime Estimation at the Time Resolution of 1 s

According to the mission profile shown in Fig. 4, the medium timescale can be discussed, where the output power cannot exactly follow the MPPT curve because of the mechanical inertia of the wind turbine, a time constant of the wind turbine at 22 s is considered [13]. On the other hand, the effects of the thermal capacitance cannot be ignored, due to the comparable magnitude of the time constant and 1 s, hence the RC thermal models are utilized to calculate the junction temperature. These two factors are different compared to the time resolution of 1 h, and more details are given as follows.

Owing to the effect of mechanical inertial, an equivalent first-order filter with a time constant is applied, the output powers with and without filtering at 10 m/s wind speed are shown in Fig. 6, it can be seen that the filtered output power is smaller than the MPPT value and a phase shift is unavoidable. It is worth mentioning that the filtered power is used for the following analysis.
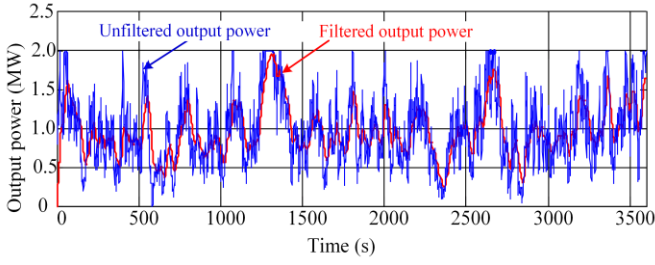
Fig. 6. Hourly output power profile at the average wind speed of 10 m/s.

Fig. 7 gives the estimation process of the consumed lifetime with the time resolution of 1 s, where the thermal model is established [14], and the Rainflow counting algorithm is used for each average wind speed profile, hence the consumed lifetime is estimated based on the Coffin-Manson model in (2) and the Miner's rule given as following:

$$CL = \sum D_v \left(k_v CL_v \right) = \sum D_v \left(k_v \frac{n_f(v)}{N_f(v)} \right) \quad (4)$$

where k_v is the coefficient to extend the damage calculation from an hour to a year and k_v=8760, D_v is the annual percentage of each wind speed obtained from the yearly wind speed mission profile shown in Fig. 2(a), and v is the wind speed corresponding to 1, 2, ..., 28 m/s.

C. Lifetime Estimation at the Time Resolution of Millisecond

For the small timescale, the short-term thermal model focuses on the thermal cycling caused by the fundamental frequency of the current. Usually, it is 50 Hz for the GSC and it ranges from zero to 15 Hz for the RSC with various wind speeds. Since the wind speed and ambient temperature are constant in this case, the mean junction temperature and junction temperature fluctuation are calculated with the Foster structure [15] at the specific wind speed:

$$T_{jm\_T/D} = P_{lossT/D} \cdot \sum_{i=1}^{4} R_{thjc\_T/D(i)} + P_{lossT/D} \cdot R_{thch\_T/D}$$
$$+ 2\left(P_{lossT} + P_{lossD} \right) R_{thhs} + T_{am} \quad (5)$$

$$dT_{j\_T/D} = 2P_{loss} \cdot \sum_{i}^{4} R_{thjc\_T/D(i)} \cdot \frac{(1 - e^{-\frac{t_{on}}{\tau_{thjc\_T/D(i)}}})^2}{1 - e^{\frac{-T_s}{\tau_{thjc\_T/D(i)}}}}$$
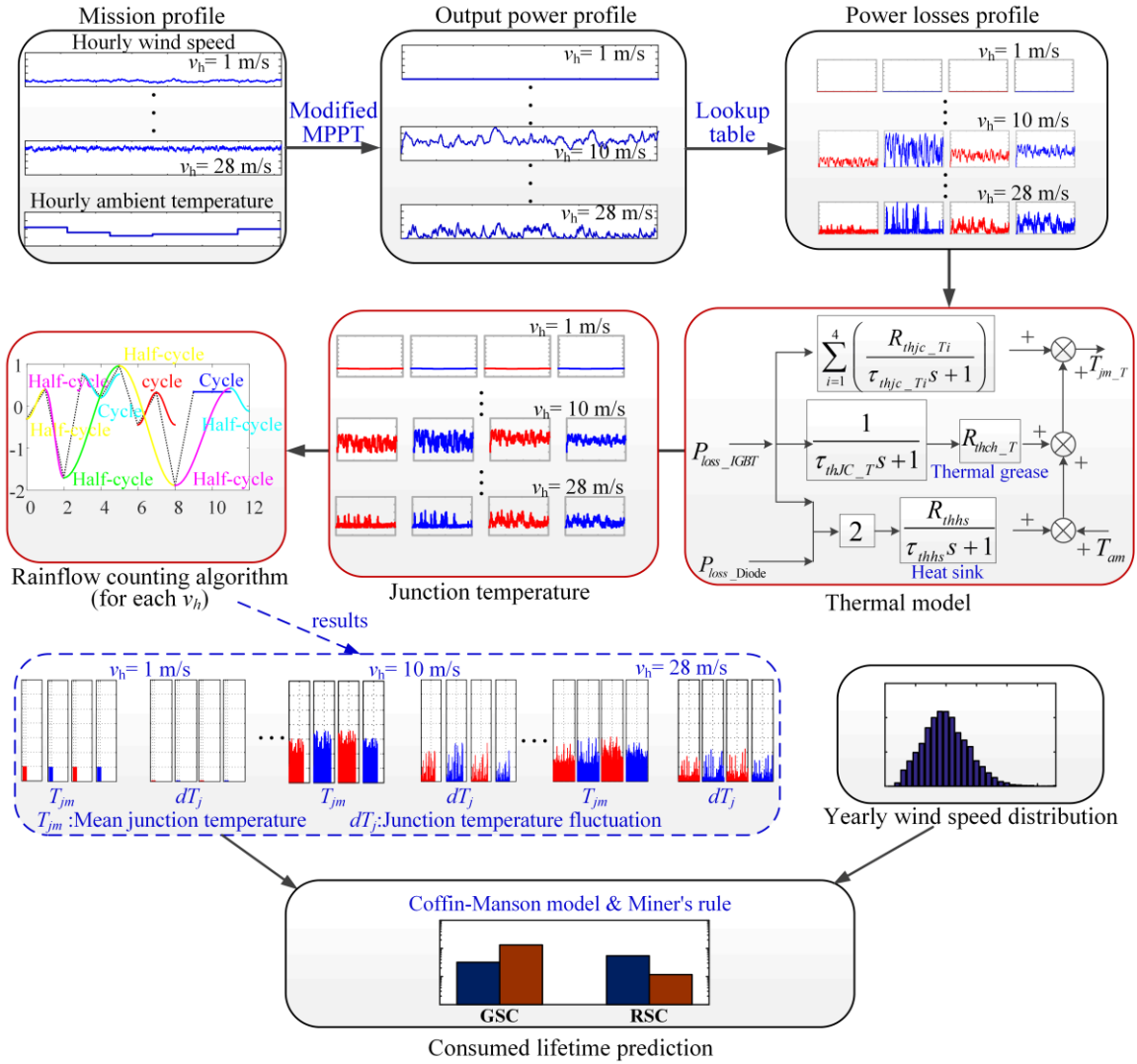

Fig. 7. The lifetime estimation procedure with the time resolution of 1 s.

where t_{on} denotes the ON-state time within each fundamental period T_s, and τ denotes each Foster layer's thermal time constant, T_{am} is 9.5 ˚C.

The estimation process at the time resolution of millisecond is shown in Fig. 8, where the output power follows the MPPT curve and the power losses are obtained by the lookup table. Moreover, the IGBTs of the GSC and the RSC have the higher power losses than that of the diodes. However, because the IGBT and the diode share the common heat sink, and the thermal grease resistance of the diode is higher than that of the IGBT, the mean junction temperature of the IGBT of the GSC and the diode of the RSC are similar. As well as the diode of the GSC and the IGBT of the RSC, they have the similar mean junction temperature. On the basis of the yearly wind speed distribution, the consumed lifetime of DFIG power converter is calculated by (2) and (4).

IV. COMPARATIVE ANALYSIS OF THE CONSUMED LIFETIME AT DIFFERENT TIMESCALES

The calculated consumed lifetime of DFIG power converter at different timescales is given in Fig. 9. In the GSC stage, the consumed lifetime of the IGBT is higher than that of the diode, hence the IGBT is more fragile than the diode in practical applications. Moreover, the consumed lifetime of the IGBT and the diode is more balanced in terms of the long-term and the medium-term thermal models, while during the short-term thermal model the ratio of the lifetime between the IGBT and the diode is almost ten times of the other two cases. In respect to the RSC stage, the diode is more fragile than the IGBT, and the ratio of the lifetime between diode and IGBT is much higher in the millisecond case than other two cases.

For the power devices of the GSC and the RSC, the consumed lifetime at different time resolutions is compared in Fig. 9(d). The long-term and medium-term thermal models dominate the total consumed lifetime of the power components of the GSC, while all the three mission profiles with the time resolutions of 1 h, 1 s, and 0.5 ms contribute to the total consumed lifetime of the power devices of the RSC. In this case, in order to reasonably obtain the lifetime of DFIG power converter, the time resolution of 1 s is appropriate when estimating the consumed lifetime of the GSC, but when calculating the consumed lifetime of the RSC, the time resolution of 0.5 ms must be considered.

The lifetime of power devices decreases with the increased time resolution, and the total consumed lifetime of the power devices is calculated by cumulating the results shown in Fig. 9. The total consumed lifetime of the diode and the IGBT of the GSC are $1.104e^{-4}$ and $3.173e^{-4}$, while they are $9.256e^{-4}$ and $1.314e^{-4}$ for the RSC. Therefore, the diode of the RSC has the highest consumed lifetime, and it dominates the lifetime of the DFIG power converter.

V. CONCLUSION

In this paper, the mission profiles (wind speed, ambient temperature) with the time resolution of one hour, one second and millisecond are discussed. For the 1 s wind speed profile, it is generated by the von Karman's spectra and an 18 % turbulence intensity is considered. Based on this, the consumed lifetime of DFIG power converter is discussed using multi-timescale thermal models. The IGBT of the GSC and the diode of the RSC are the most fragile components regardless of the time resolutions, and the consumed lifetime of the diode of the RSC is the highest because of a high junction temperature fluctuation. For the GSC, the low-resolution and medium-
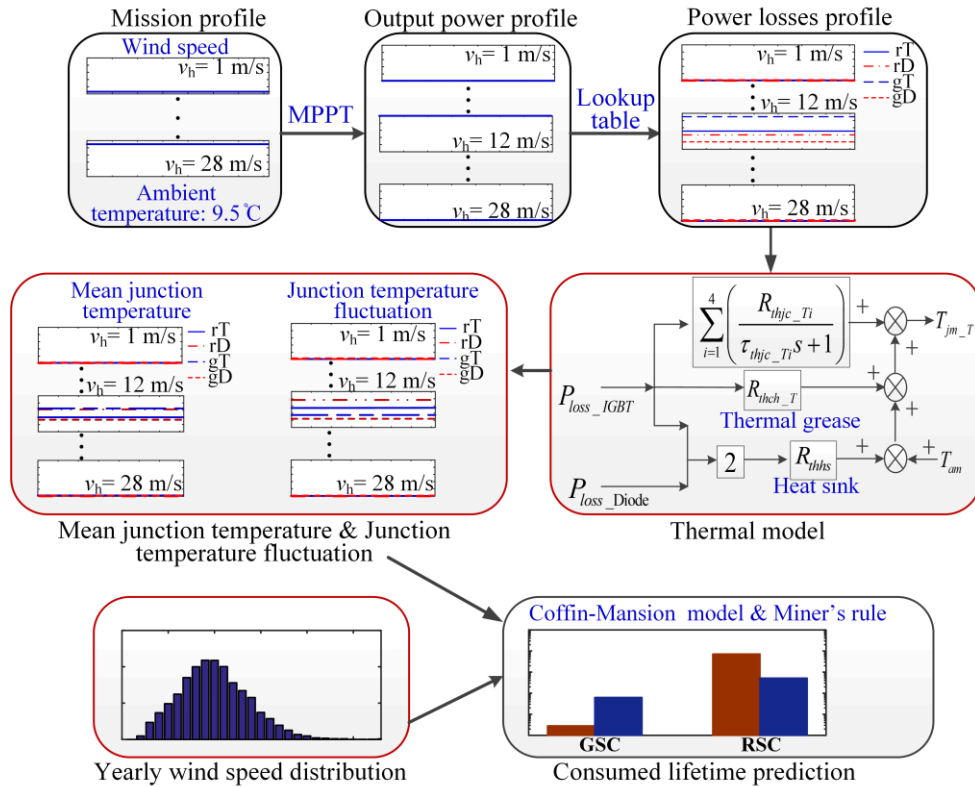

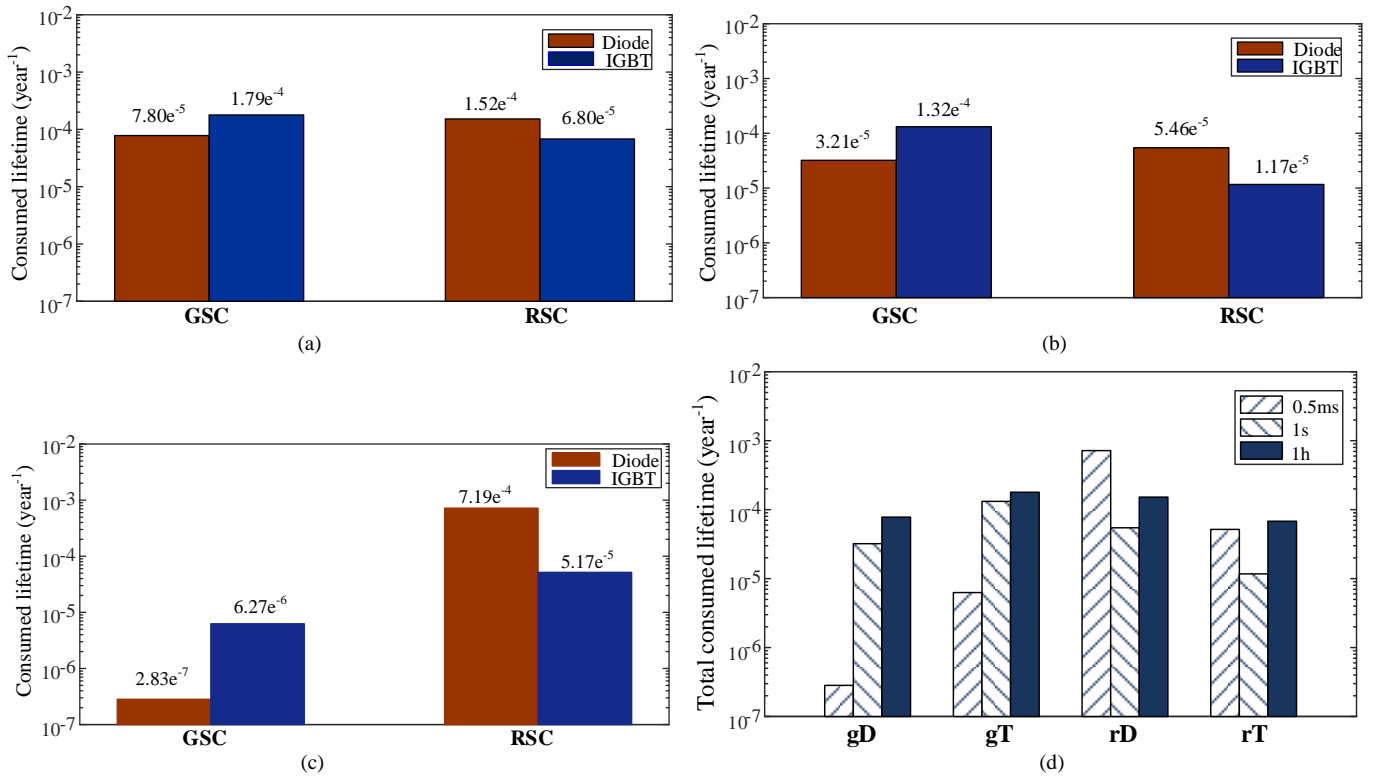Fig. 8. The lifetime estimation procedure with the time resolution of 0.5 ms.

Fig. 9. The consumed lifetime of the DFIG power converter with different time resolutions: (a) 1 *h*, (b) 1 *s*, (c) 0.5 *ms*, and (d) total consumed lifetime.

resolution consume the similar magnitude of the lifetime, while the high-resolution consumes much less. For the RSC, the low-resolution, medium-resolution, and high-solution almost consume the same magnitude of the lifetime. The results shown in this paper provide a guidance for the DFIG power converter design, and the more frequent maintenance is required for the diode of the GSC and the IGBT of the RSC.

REFERENCES

[1] S. Yang, A. Bryant, P. Mawby, D. Xiang, R. Li, and P. Tavner, "An Industry-Based Survey of Reliability in Power Electronic Converters," *IEEE Transactions on Industry Applications*, vol. 47, no. 3, pp. 1441-1451, Mar. 2011.

[2] F. Blaabjerg, M. Liserre, and K. Ma, "Power electronics converters for wind turbine systems," *IEEE Transactions on Industry Applications*, vol. 48, no. 2, pp. 708-719, Dec. 2011.

[3] H. Wang, M. Liserre, and F. Blaabjerg, "Toward reliable power electronics: Challenges, design tools, and opportunities," *IEEE Industrial Electronics Magazine*, vo. 7, no. 2, pp. 17-26, Jun. 2013.

[4] D. Zhou, F. Blaabjerg, M. Lau, and M. Tonnes, "Optimized reactive power flow of DFIG power converters for better reliability performance considering grid codes," *IEEE Transactions on Industrial Electronics*, vol. 62, no. 3, pp. 1552-1562, Oct. 2015.

[5] R. Billinton and W. Wangdee, "Reliability-based transmission reinforcement planning associated with large-scale wind farms,". *IEEE Transactions on Power Systems*, vol. 22, no. 1, pp. 34-41, Jan. 2013

[6] F. Blaabjerg, Y. Yang, D. Yang, and X. Wang, "Distributed power-generation systems and protection," *in Proceedings of the IEEE*, vol. 105, no. 7, pp. 1311-1331, Jul. 2017.

[7] J. Ying, X. Yuan, and J. Hu, "Inertia Characteristic of DFIG-based WT under Transient Control and Its Impact on the First-Swing Stability of SGs," *IEEE Transactions on Energy Conversion*, early access.2017.doi: 10.1109/TEC.2017.2698521.

[8] K. Ma and F. Blaabjerg, "Multi-timescale modelling for the loading behaviors of power electronics converter", *in IEEE 2015 Energy Conversion Congress and Exposition*, pp. 5749-5756, 2015.

[9] T. Burton, N. Jenkins, D. Sharpe, and E. Bossanyi, "Wind energy handbook", *John Wiley & Sons*, 2011.

[10] C. Nichita, D. Luca, B. Dakyo and E. Ceanga, "Large band simulation of the wind speed for real time wind turbine simulators," *IEEE Transactions on Energy Conversion*, vol. 17, no. 4, pp. 523-529, Dec. 2002.

[11] G. Zhang, D. Zhou, J. Yang and F. Blaabjerg, "Fundamental-frequency and load-varying thermal cycles effects on lifetime estimation of DFIG power converter," *Microelectronics Reliability*, vol. 76, pp. 549-555, 2017.

[12] R. Bayerer, T. Herrmann, T. Licht, J. Lutz, and M. Feller, "Model for power cycling lifetime of IGBT modules-various factors influencing lifetime", *in International Conference on Integrated Power Systems (CIPS)*, pp. 1-6, 2008.

[13] C. Tang, M. Pathmanathan, W.L. Soong and N. Ertugrul, "Effects of inertia on dynamic performance of wind turbines", *in IEEE Power Engineering Conference*, pp. 1-6, 2008.

[14] K. Ma, N. He, M. Liserre, and F. Blaabjerg, "Frequency-domain thermal modeling and characterization of power semiconductor devices," *IEEE Transactions on Power Electronics*, vol. 31, no. 10, pp. 7183-7193, 2016.

[15] "Thermal equivalent circuit models," *Infineon Application Note AN* 2008-03, Jun. 2008.